Roothairless5, which functions in maize (Zea mays L.) root hair initiation and elongation encodes a monocot-specific NADPH oxidase

Josefine Nestler, Sanzhen Liu, Tsui-Jung Wen, Anja Paschold, Caroline Marcon, Ho Man Tang, Delin Li, Li Li, Robert B. Meeley, Hajime Sakai, Wesley Bruce, Patrick S. Schnable, and Frank Hochholdinger

Published Version Information

Citation: Nestler, J., Liu, S., Wen, T. -., Paschold, A., Marcon, C., Tang, H. M., et al. (2014). Roothairless5, which functions in maize (zea mays L.) root hair initiation and elongation encodes a monocot-specific NADPH oxidase. Plant Journal, 79(5), 729-740.

Digital Object Identifier (DOI): 10.1111/tpj.12578

Publisher's Link: http://onlinelibrary.wiley.com/doi/10.1111/tpj.12578/abstract

Roothairless5, which functions in maize (*Zea mays* L.) root hair initiation and elongation encodes a monocot-specific NADPH oxidase

Josefine Nestler[1,2,*], Sanzhen Liu[3,4*], Tsui-Jung Wen[5,6], Anja Paschold[1], Caroline Marcon[1], Ho Man Tang[6,7], Delin Li[8], Li Li[3,9], Robert B. Meeley[10], Hajime Sakai[11], Wesley Bruce[10,12], Patrick S. Schnable[3,8,13,‡], Frank Hochholdinger[1,‡]

[1] *Institute of Crop Science and Resource Conservation, Crop Functional Genomics, University of Bonn, 53113 Bonn, Germany*

[2] *Current address: Crop, Environment and Livestock Division, Japan International Center for Agricultural Sciences (JIRCAS), Tsukuba, Ibaraki 305-8686, Japan*

[3] *Department of Agronomy, Iowa State University, Ames, IA 50011-3650, USA*

[4] *Department of Plant Pathology, Kansas State University, Manhattan, KS 66506-5502, USA*

[5] *Current address: Redmond, WA 98052, USA*

[6] *Department of Genetics, Development, and Cell Biology, Iowa State University, Ames, IA 50011-3650, USA*

[7] *Current Address: Center for Cell Dynamics, Department of Biological Chemistry, Johns Hopkins University School of Medicine, Baltimore, MD 21205, USA*

[8] *Department of Plant Genetics & Breeding, China Agricultural University, Beijing 100193, China*

[9] *College of Agronomy, Northwest A&F University, Yangling 712100, China*

[10] *Pioneer Hi-Bred International, Inc. - A DuPont Company, Johnston, IA 50131-0184, USA*

[11] *DuPont Crop Genetics Research, Experimental Station, PO Box 80353, Wilmington, DE 19880-0353, USA*

[12] *Current address: BASF, Research Triangle Park, NC 27709, USA*

[13] *Center for Plant Genomics, Iowa State University, Ames, IA 50011-3650, USA*

[*] These authors contributed equally to this study

‡ Corresponding authors:

Frank Hochholdinger
INRES, Crop Functional Genomics, University of Bonn
Friedrich-Ebert-Allee 144, 53113 Bonn, Germany
Email: hochholdinger@uni-bonn.de
Tel: +49 228 73 60334
Fax: +49 228 73 60333

Patrick S. Schnable
2035B Roy J. Carver Co-Lab
Iowa State University
Ames, Iowa 50011-3650
Email: schnable@iastate.edu
Tel: +1 515 294 0975
Fax: +1 515 294 5256

E-mail addresses of all authors:
Josefine Nestler: jnestler@affrc.go.jp
Sanzhen Liu: liu3zhen@ksu.edu
Tsui Jung Wen: tjkwen@gmail.com
Anja Paschold: paschold@uni-bonn.de
Caroline Marcon: marcon@uni-bonn.de
Ho Man Tang: hollytang@gmail.com
Delin Li: delin.bio@gmail.com
Li Li: lli1204@iastate.edu
Robert B. Meeley: bob.meeley@pioneer.com
Hajime Sakai: hajime.sakai@cgr.dupont.com
Wesley Bruce: wes.bruce@basf.com
Patrick S. Schnable: schnable@iastate.edu
Frank Hochholdinger: hochholdinger@uni-bonn.de

Running title: *roothairless5* encodes a NADPH oxidase

Keywords: maize / root hairs / *rth5* / NADPH oxidase / RNA-Seq

Word count:

Summary: 207

Introduction: 785

Results: 1578

Discussion: 2102

Experimental procedures: 1649

Acknowledgements: 68

Figure legends: 556

Total: 6945

Abstract

Root hairs are instrumental for nutrient uptake in monocot cereals. The maize (*Zea mays* L.) *roothairless5* (*rth5*) mutant displays defects in root hair initiation and elongation manifested by a reduced density and length of root hairs. Map-based cloning revealed that the *rth5* gene encodes a monocot-specific NADPH oxidase. RNA-Seq, *in situ* hybridization and qRT-PCR experiments demonstrated that the *rth5* gene displays preferential expression in root hairs but also accumulates to low levels in other tissues. Immunolocalization detected RTH5 proteins in the epidermis of the elongation and differentiation zone of primary roots. Because superoxide and hydrogen peroxide levels are reduced in the tips of growing *rth5* mutant root hairs as compared to wild-type, and ROS is known to be involved in tip growth, we hypothesize that the RTH5 protein is responsible for establishing the high levels of ROS in the tips of growing root hairs required for elongation. Consistent with this hypothesis, a comparative RNA-Seq analysis of 6-day-old *rth5* versus wild-type primary roots, revealed significant over-representation of only two gene ontology (GO) classes related to the biological functions (i.e., oxidation/reduction and carbohydrate metabolism) among 893 differentially expressed genes (FDR <5%). Within these two classes the subgroups “response to oxidative stress” and “cellulose biosynthesis” were most prominently represented.

Introduction

Root hairs consist of tubular extensions of epidermis cells and comprise up to 77% of the root surface of cereals (Parker *et al.* 2000). They are therefore considered to be instrumental for nutrient uptake and to support plant growth and development (Gilroy and Jones 2000), a view that is supported by replicated field trials involving near-isogenic lines of the maize *roothairless 3* mutant, which conferred significant losses in grain yield (Hochholdinger *et al*. 2008).

Generally, root hair bearing epidermis cells (trichoblasts) are short and contain denser cytoplasm, whereas non-root hair forming cells (atrichoblasts) are long and contain large vacuoles (Cormack, 1947). Several types of root hair patterning have been described. In dicot species such as *Arabidopsis thaliana*, position-dependent root hair initiation leads to alternating longitudinal files of trichoblasts and atrichoblasts (Schiefelbein and Somerville 1990). In contrast, some monocot species such as rice form trichoblasts via asymmetric cell divisions. Finally, random, unpredictable initiation without development of cytologically detectable distinct atrichoblasts and trichoblasts is observed in some mono- and dicot species such as maize and soybean (Clowes 2000).

In Arabidopsis, epidermis cells overlaying two cortical cells (H cell position) develop into trichoblasts which give rise to root hairs. Cells overlaying only one cortical cell (N cell position) differentiate into hairless atrichoblasts (Schiefelbein and Somerville 1990). In Arabidopsis, the molecular network involved in epidermis specification and thus root hair initiation is well understood (Dolan 2001, Hochholdinger and Nestler 2012, Ishida *et al.* 2008). The Arabidopsis homeodomain transcription factor GLABRA2 (GL2) which is specifically expressed in atrichoblasts inhibits the expression of genes responsible for root hair formation (Masucci *et al.* 1996). GL2 expression is activated by WEREWOLF (WER), a MYB-like transcription factor (Lee and Schiefelbein 1999). The homologous MYB-like transcription factor CAPRICE (CPC) replaces WER in trichoblasts. CPC does not contain an activation domain and can therefore not activate *Gl2* expression (Wada *et al.* 2002).

Root hair growth is divided into three phases: first, defined swelling to form a bulge, second, transition to tip growth and finally tip growth by oriented exocytosis (Dolan *et al.* 1994). Recently, root hair formation from initiation to elongation in Arabidopsis was characterized via genome-wide transcriptome analyses of wild-type and 17 mutant lines leading to a complex model of transcriptional regulation (Bruex *et al.* 2012).

Reactive oxygen species (ROS) and ROS-related proteins play an important role in root hair tip growth. Superoxide is produced by NADPH oxidases (NOXs) using oxygen as electron donor (Gapper and Dolan 2006). Plant NADPH oxidases were identified as homologs of the mammalian gp91^{phox}, the catalytic subunit of the phagocyte NADPH oxidase, and named respiratory burst oxidase homologs (RBOHs) (Torres *et al.* 1998). To date, the most thoroughly investigated *rboh* gene is *AtrbohC* or *ROOTHAIR DEFECTIVE 2* (*RHD2*) of Arabidopsis, which is involved in establishing hydrogen peroxide and superoxide peaks in growing root hair tips (Foreman *et al.* 2003). The *rhd2* mutant lacks these high hydrogen peroxide and superoxide concentrations and the associated cytoplasmic Ca^{2+} influx (Wymer *et al.* 1997). The membrane localized RHD2 protein is activated by Ca^{2+} (Takeda *et al.* 2008). Although root hair bulges form in *rhd2* mutants they do not elongate (Schiefelbein and Somerville 1990). Recently, it was demonstrated that *rhd2* mutants form macrotubules leading to a disturbance in mitosis in the root tip (Livanos *et al.* 2012). In addition, the potential functions in root and root hair growth, several putative functions in shoot tissues and plant immune response have been assigned to *rboh* genes (Galletti *et al.* 2008, Kwak *et al.* 2003, Lin *et al.* 2009, Wi *et al.* 2012, Wong *et al.* 2007, Yamauchi *et al.* 2011, Yi *et al.* 2010).

In maize, only a few mutants defective in root hair formation have been isolated. Two pleiotropic mutants, *disorganized aleurone layer 1* and *2* (*dil1* & *dil2*) display in addition to other developmental defects fewer root hairs and aberrant root hair morphology (Lid *et al.* 2004). Three *roothairless* mutants (*rth1* to *rth3)* are defective at different stages of root hair formation (Wen *et al.* 1994). Thus far only two maize genes involved in root hair elongation have been cloned. Mutants of the r*oothairless1* (*rth1*) gene condition short root hairs and a dwarf plant phenotype (Wen and Schnable 1994) due to a defect in the encoded SEC homolog involved in polar exocytosis (Wen *et al.* 2005). *Roothairless3* (*rth3*) encodes a monocot specific COBRA-like protein that participates in cell wall expansion and biosynthesis (Hochholdinger *et al.* 2008); mutants in this gene result in very short root hairs defective in bulge formation (Wen *et al*. 1994).

Here we describe the identification, cloning and characterization of the maize *roothairless5* gene controlling root hair initiation and outgrowth which encodes a monocot-specific NADPH oxidase involved in superoxide production.

Results

The *roothairless5* gene controls both root hair length and density

An EMS mutagenesis screen yielded a recessive mutant (Schnable Lab Accession # 1350) that affects root hair development but has no other obvious effects on plant growth and development. Genetic crosses demonstrated that this mutant is not allelic to the previously described mutants *rth1*, *rth2* and *rth3* (Wen *et al*. 1994). The affected gene and reference allele were designated *rth5* and *rth5-1*, respectively. Compared to wild-type (Figure 1A and 1C), the *rth5* mutant displays significantly shorter root hairs (Figure 1B and 1D). Root hair length and density of wild-type and *rth5* primary roots were analyzed via eSEM (environmental scanning electron microscopy). The length of root hairs on primary roots of 4-day-old (4 d) *rth5* mutants was decreased to 4% of wild-type length (Figure 1E). Moreover, root hair density of mutants was reduced to 64% of wild-type density (Figure 1F). In 10 d seedlings it is possible to observe root hairs on seminal and shoot-borne roots and the length and number of root hairs on these roots are also reduced in the mutant (Figure S1).

Map-based cloning of *rth5* identified an NADPH oxidase

Using Sequenom-based bulked segregant analysis (BSA) (Liu *et al*. 2010) the *rth5* locus was mapped to the long arm of chromosome 3. By analyzing F_2 and F_1BC populations (Methods) the *rth5* gene was mapped to the interval 180.1-180.4 Mb of chromosome 3 (assembly version: ZmB73_AGPv1 release 4a53; http://ftp.maizesequence.org/release-4a.53/), flanked by IDP (insertion deletion polymorphism) markers IDP4064 and C3.184743 (Figure 2A). This interval harbors only five gene models, including GRMZM2G426953, encoding an NADPH oxidase (NOX), which contains a G to A transition at position 2462, resulting in a cysteine (C) to tyrosine (Y) conversion at amino acid position 821 close to the C-terminus of the protein (Figure 2B). This amino acid exchange is the result of a G-to-A transition relative to the B73 allele, which is characteristic of EMS-induced mutations. .

The affected cysteine residue is also conserved among divergent NADPH oxidases ranging from plants to yeast and human (Figure 2C). Hence, an alteration of this conserved residue in the predicted NAD substrate binding region might lead to a functional deficiency in the *rth5* mutant.

Confirmation of *rth5* identity via the generation of independent alleles

To confirm that the mutation in candidate gene GRMZM2G426953 indeed confers the phenotype of the *rth5* mutant, several independent putative *Mutator* alleles were isolated from Pioneer´s trait utility system of corn (TUSC, Bensen *et al*. 1995). Among these putative *Mu* insertion alleles, three displayed the roothairless phenotype and each of these alleles contained a *Mutator* insertion in the candidate gene as demonstrated by sequencing. Allele *rth5-3* contains a *Mu1* insertion in exon 5 (Figure 2B) while *rth5-2* and *rth5-4* contain *MuDR* insertions in exons 3 and 5, respectively (Figure 2B).

The gene structure

The B73 allele of the *rth5* gene consists of 14 exons and 13 introns (Figure 2B) encoding a 3,792 bp mRNA (including 5' and 3' UTR). This mRNA encodes an 852 amino acid protein with a predicted molecular weight of ~96 kDa.

The RTH5 protein is predicted to contain four trans-membrane (TM) domains, two EF hand motifs, FAD and NAD cofactor binding sites, a ferric reductase domain, and the NADPH oxidase characteristic for NADPH oxidases (Figure 2B).

The NADPH oxidase family in maize

Based on sequence similarity with the RTH5 protein 17 respiratory burst oxidase homologs (*rboh*) genes were identified in the maize filtered gene set (FGS, release: 4a53; http://ftp.maizesequence.org/release-4a.53/filtered-set/), a set of high confidence gene models. Phylogenetic reconstructions based on the full-length protein sequences of all known members of the maize, Arabidopsis, soybean and rice NADPH oxidase gene families (Figure 3) were performed. Two major groups of NADPH oxidases were observed. All NADPH oxidases exhibit diverse sequences in their N-terminus. The smaller group II is characterized by less conservation or the absence of the NADPH oxidase domain and a different conserved sequence in the NAD cofactor binding region (Figure S2). Interestingly, no soybean and only one rice and maize protein were included in group II, whereas eight Arabidopsis RBOH proteins belong to that subgroup. Along with two other maize and two rice RBOHs RTH5 is a member of a monocot-specific sub-clade of group I (Figure 3). No homeolog of RTH5 resulting from an ancient genome duplication was found in the maize genome. *In silico* searches for syntenic

homologs (genomeevolution.org/CoGe) identified the rice gene Os01g61880, which was also the closest homolog of RTH5 in the phylogenetic tree (Figure 3). RTH5 and its two closest maize homologs RBOH11 and RBOH13 are located in a subgroup of the phylogenetic tree characterized by the presence of a few additional amino acids at the end of the FAD cofactor binding site (Figure S2).

***The rth5 gene* is preferentially expressed in root hairs**

Tissue specific expression of *rth5* and all 17 *rboh* family members was examined via qRT-PCR in six different seedling tissues including the cap of the primary root, elongation zone, differentiation zone without root hairs, isolated root hairs, the coleoptilar node and the first leaf. *Rth5* transcripts accumulated in all tested tissues, but the significantly highest level was detected in root hairs (Figure 4B). Expression data of the remaining *rboh* family members in these tissues are summarized in Figure S3. Moreover, the qTeller tool (www.qteller.com) was used to compare the accumulation of *rth5* transcripts in RNA-Seq data from a wide range of tissues and organs. The highest expression values were observed in seedling roots (Figure S4). The relative expression levels of all 17 *rboh* genes in root hairs were determined via quantitative real time PCR (qRT-PCR). The *rth5* gene displayed the highest expression, accounting for 52% of the total *rboh* expression in maize root hairs (Figure 4A). The genes *rboh11* and *rboh13,* the closest homologs of *rth5* were only very weakly expressed in root hairs.

RNA *in situ* hybridization experiments were used to study root tissue specific expression patterns. Cross sections hybridized with an *in vitro* transcribed *rth5* RNA antisense probe resulted in a signal in root hairs whereas the sense probe yielded no signal (Figure 4C and 4D).

The RTH5 protein is localized in epidermal cells of the primary root

Immunohistochemical experiments were performed to localize the RTH5 protein *in situ* (Figure 4E to 4J). In cross sections of the differentiation zone, RTH5 antibody signals were detected in all epidermis cells and in root hairs (Figure 4E), whereas the control sections displayed no signal (Figure 4F).

In longitudinal sections an RTH5 signal was detected in root hairs and all epidermis cells of the root hair zone (Figure 4G). Interestingly, an RTH5 signal was also detected in longitudinal

sections of the elongation zone, which does not form root hairs (Figure 4I). The control sections, showed no detectable color reaction (Figure 4H & 4J).

Both, cross- and longitudinal sections displayed no difference in signal intensity or tissue organization between *rth5* and wild-type apart from the root hair defect (Figure S5).

The *rth5* mutant accumulates less ROS during root hair tip growth

Superoxide is a very short-lived radical that is rapidly converted into hydrogen peroxide (Figure 5A). Staining for both molecules was performed in wild-type and *rth5* mutant seedlings (Figure 5B) by NBT for superoxide and DAB and H_2DCF-DA for hydrogen peroxide. NBT and DAB exclusively stained root hair cells, while H2DCF-DA also exhibited the highest intensity of fluorescence in root hairs but also slightly stained other epidermis cells upon longer incubation. Subsequently, presence or absence of high ROS signals in root hair tips were quantified (Figure 5C). While 74% of wild-type root hairs displayed the superoxide (NBT) signal at the tip, the frequency of a tip-high signal was significantly reduced to 24% in *rth5* root hairs. Similarly, 77% and 71% of wild-type root hairs exhibited a high hydrogen peroxide signal in the tips of root hairs as detected by DAB or H_2DCF-DA, respectively, while only 27% and 21% of *rth5* root hairs displayed this signal specifically in root tips (Fig. 5C). Fisher´s exact test showed that these differences were significant at $p \leq 0.001$.

RNA-Seq of *rth5* mutants vs. wild-type

To understand the influence of *rth5* on global patterns of transcription, RNA-Seq was performed on 6-day-old roots from the *rth5* mutant and wild-type seedlings (Methods). Two biological replicates were analyzed for each genotype. Approximately 98% of raw reads from each sample passed the quality check and trimming procedure. 3.7-4.7 million reads per replicate (~88% of the post-trimmed reads) were uniquely and confidently mapped to the B73 reference genome (Table S2) (Methods). Among 21,007 genes that have a total of ≥20 RNA-Seq reads summed across all four biological replicates, 893 differentially expressed genes were identified at a false discovery rate (FDR) >5%. Among those, 444 genes were preferentially expressed in wild-type primary roots, including 100 genes displaying a fold-change (Fc) ≥2. Moreover, 449 genes were preferentially expressed in *rth5* primary roots including 195 genes displaying a Fc ≥2 (Table S3, Figure S6). A gene ontology (GO) enrichment analysis of the 893 differentially expressed genes

revealed statistically significant over-representation of three GO terms related to “oxidation/reduction” and six GO terms related to “carbohydrate metabolism” (Table S4). The “oxidation/reduction” category contained four differentially expressed *rboh* genes, including *rth5*. While the *rth5* gene (GRMZM2G426953) was preferentially expressed in wild-type versus mutant primary roots (Fc: 1.4), the genes *rboh7* (GRMZM2G065144), *rboh6* (GRMZM2G034896) and *rbohAlike* (GRMZM2G037993) were preferentially expressed in mutant *rth5* roots. The relation of the “oxidation/reduction” and “carbohydrate metabolism” subgroups are summarized in Tables S5 and S6, respectively. Within these two classes, the subgroups “response to oxidative stress” and “cellulose biosynthesis” were most prominently represented. Overall, these RNA-Seq results are consistent with the view that *rth5/rbohA* functions in producing ROS (“response to oxidative stress”) required for elongation (“cellulose biosynthesis”) of root hairs.

Discussion

The maize *rth5* mutant displays significantly shortened root hairs and reduced root hair density while aboveground development remains unaffected. Hence, *rth5* specifically controls both the elongation of root hairs and the specification of epidermis cells or the initiation of root hairs. More specifically, root hair elongation in the mutant *rth5* is affected during the transition from bulge to tip growth. In contrast to *rth5*, root hairs of the *rth3* mutant are characterized by disrupted bulges while *rth1* and *rth2* root hairs fail to elongate after transition to tip growth (Wen and Schnable 1994). The *rth5* mutant resembles the phenotype of *rth2* and *rth3* (Wen and Schnable 1994), which are specifically affected in root hair formation. In contrast, the maize mutants *rth1* (Wen and Schnable 1994), *dil1* and *dil2* (Lid et al., 2004) which are defective in root hair formation also display pleiotropic effects during development. The *rth1* mutant displays general growth abnormalities during development (Wen *et al*. 1994) while *dil1* and *dil2* control cell division orientation in the aleurone, leaf and root epidermis. The maize mutant *rth5* forms fewer root hairs as compared to wild-type primary roots suggesting that the *rth5* gene is involved not only in root hair elongation but also in epidermis specification and/or root hair initiation.

In *rth5*, all root types including primary, seminal, lateral, and shoot-borne roots display defects in root hair formation, suggesting that the RTH5 protein is critical for root hair formation in all root types. A general defect in root hair formation affecting all root types has also been observed for the *rth1*, *rth2* and *rth3* mutants (Hochholdinger *et al.* 2008, Wen *et al.* 1994). In contrast to this general mechanism of root hair formation in all root types, the control of lateral root formation is root type-specific. For instance *rum1* (Woll *et al.* 2005) and *lrt1* (Hochholdinger and Feix 1998) display root type-specific defects which are confined to embryonic roots. In these mutants postembryonic shoot-borne roots do not display any lateral root defects.

The RTH5 protein is characterized by several functional domains (Figure 2B) including four trans-membrane domains, responsible for the membrane embedding and two EF hand motifs, which are required for Ca^{2+} regulation. Moreover, the FAD and NAD domains confer binding to the cofactor FAD and the substrate NADPH, respectively. Regulation of the RBOHA/RTH5 NADPH-oxidase by a mitogen-activated protein kinase cascade controlled by abscisic acid signalling was demonstrated in maize leaves (Lin *et al*. 2009).

Based on the identification of the co-factor binding site and the functional assignment, the *rth5* gene is predicted to encode a NADPH oxidase (NOX). The NOX protein family is present in most eukaryotic species (Bedard *et al.* 2007). The *rth5* mutant was induced by EMS, which resulted in a guanine to adenine substitution in the genomic sequence changing the cysteine (C) residue in amino acid position 821 to tyrosine (Y) (Figure 2B). Cysteine residues often form intra- or inter protein disulfide bridges to enable secondary structures. As this cysteine residue is highly conserved among a very diverse set of species (Figure 2C) it is likely that the C821Y mutation is disabling a functionally important protein domain. A point mutation of this conserved C in the human NADPH oxidase 2 (*NOX2*) gene results in the genetic disorder chronic granulomatous disease (Kawahara *et al.* 2007). This disease affects cells of the immune system which have difficulties in forming reactive oxygen compounds, including superoxide used to kill certain ingested pathogens.

Phylogenetic reconstruction of RBOH (RESPIRATORY BURST OXIDASE HOMOLOG) proteins of rice, maize, soybean, and Arabidopsis revealed the existence of two subgroups. These subgroups are distinguished based on differences in the sequences of the NAD binding region, which are conserved within each group (Figure S2). Ten Arabidopsis RBOH proteins are classified to group I, which is consistent with previous annotations of superoxide producing NOX proteins (Kawahara *et al*. 2007). Interestingly, all soybean proteins are assigned to group I, while eight of 18 members of the Arabidopsis RBOH protein family are classified in group II. According to their annotation, group II proteins are often connected to iron deficiency and might function as ferric reductases which are NOX proteins that do not produce superoxide (Ivanov *et al.* 2012).

The nine members of the group I subclade that includes RTH5 are characterized by nine additional amino acids in the FAD cofactor domain as compared to the remaining group I proteins. The five monocot-specific proteins in this subclade lack 15 amino acids in their NADPH binding region. Both, the additional amino acids in the FAD, and the missing amino acids in the NAD region might confer altered binding to cofactors or substrates leading to specialized functions.

While several types of NOX proteins are found in mammals ranging from ancestral types to peroxidase containing DUOXs, in plants only homologs of EF-hand-containing NOX5-types have been identified (Bedard *et al*. 2007). Human NOX proteins consist of two trans-membrane

heterodimers (gp91^{phox} and p22^{phox}) and four regulatory subunits (p40^{phox}, p47^{phox}, p67^{phox}, and Rac2) in the cytoplasm (Lam *et al.* 2010). Thus far, no homologs for the regulatory subunits p47^{phox}, p67^{phox}, or p22^{phox} have been found in plants (Bedard *et al.* 2007).

The human NOX2 have been shown to play a role in the production of superoxide as a first defense response to microorganisms invading neutrophils and macrophages (Lam *et al*. 2010, Nauseef 2008). Plant NOX proteins have been shown to function in plant immunity and several developmental processes. Pepper and tobacco NOX proteins were demonstrated to function in plant immunity (Wi *et al*. 2012, Yi *et al*. 2010). Aerchenyma formation after waterlogging was shown to be conferred by the maize NOX protein GRMZM2G300965 (Yamauchi *et al*. 2011), which showed specific expression in the root cap and the elongation zone (Figure S4, RBOH10). Finally, Arabidopsis RBOHD and RBOHF are involved in ABA-dependent stomata closure (Kwak *et al*. 2003) and lead to an oxidative burst following infection (Galletti *et al.* 2008).

The Arabidopsis RBOH protein RBOHC (RHD2), which is distantly related to RTH5 also controls root hair growth. Arabidopsis plants defective in *RHD2* gene function form very short root hairs that do initiate bulges which do not elongate (Schiefelbein and Somerville 1990). Moreover, such plants display stunted root growth (Foreman *et al*. 2003), an effect that was not observed for *rth5* mutant roots. *RHD2* is expressed in root epidermal cells, but also in the cortical cells of the elongation- and differentiation zone (Foreman *et al*. 2003).

Consistent with its mutation in the C-terminus of the protein, the expression of the *rth5-1* mutant reference allele was only slightly reduced as compared to wild-type primary roots (Figure S5). Similarly, protein levels detected by immunohistochemistry and Western blot analyses did not show any obvious change between wild-type and *rth5-1* mutants (see Figure 4 and Figure S5). Although expression and protein abundance are not dramatically affected, this mutation significantly affects the function of the protein as illustrated by the mutant phenotype.

Expression of *rth5* was detected in several shoot and root tissues at low levels with expression maxima in root hairs (Figure 4 and Figure S4). Similarly, the rice *rboh* genes are also expressed in multiple plant organs and tissues (Wong *et al.* 2007). In maize root hairs *the rth5* gene accounts for 52% of the expression of all 17 *rboh* genes and hence the majority of NADPH oxidase transcripts in root hairs. The RTH5 protein was detected preferentially in root hairs and epidermis cells but weaker signals were also detected in root cortex cells (Figure 4). In two studies mainly focusing on the influence of hormones on NADPH oxidase activity in maize

leaves it was demonstrated that expression of *rth5* (*rbohA*) is induced after abscisic acid and brassinosteroid treatment as well as hydrogen peroxide application (Lin *et al*.2009, Zhang *et al.* 2010). These experiments suggest that RTH5 may play a role in hormone-mediated oxidative defense in leaves. Further analyses will be required to determine whether RTH5 plays a similar role in roots, in addition to its known roles in root hair initiation and elongation.

Arabidopsis root hairs display high Ca^{2+} and superoxide concentrations in their growing tips (Foreman *et al*. 2003). The tips of root hairs of the mutant *rth5* displayed significantly less superoxide staining and accumulate less hydrogen peroxide than wild-type plants (Figure 5). These results suggest that as a consequence of a functional defect of the RTH5 protein the *rth5* mutant is unable to establish high levels of ROS in the tips of root hairs. Not all growing tips of wild-type root hairs displayed staining for superoxide and hydrogen peroxide. Some root hairs may have died during the staining procedure; some may not have taken up the indicator chemicals. Consistent with expression data the presence of RTH5 homologous RBOH proteins may account for the residual ROS content detected in the mutant (Figure S3).

A model for the function of RTH5 in root hair elongation is summarized in Figure 6A. Superoxide molecules in the root hair tips produced by RTH5 are transformed rapidly into hydrogen peroxide, which in turn is converted to hydroxyl radicals by apoplastic peroxidases (Liszkay *et al.* 2003). These hydroxyl radicals are cleaving polysaccharides (Fry 1998) and therefore cause cell wall loosening, thereby enabling polarized cell growth (Bibikova *et al.* 1998, Liszkay *et al.* 2004).

In Arabidopsis the molecular interactions resulting in position-dependent root hair initiation are well characterized (reviewed in: Hochholdinger and Nestler 2012). In contrast, the molecular network underlying random root hair patterning in maize remains enigmatic (Clowes 2000). The reduced root hair density observed in mutant seedlings suggests that RTH5 is involved not only in root hair tip growth, but also in root hair initiation or epidermis specification. The presence of RTH5 in all epidermal cells is consistent with the hypothesis that superoxide is only produced upon activation of RTH5 which thus acts as a signal converter, similar to the human NOX2 (Lam *et al*. 2010), which subsequently promotes root hair initiation. This is supported by the finding of selective root hair cell superoxide staining in the maize differentiation zone. In contrast, all epidermis cells display superoxide staining in the elongation zone (Liszkay *et al*. 2004). To act in root hair initiation, we hypothesize that a yet unknown root hair initiation signal molecule

activates RTH5 mediated superoxide production, leading to both the establishing of root hairs and their subsequent elongation. Residual root hair initiation in the *rth5* mutant might be controlled by RTH5-independent pathways. Due to the lack of functional RTH5 proteins these root hairs fail the transition to tip growth.

The human small GTPase RAC2 is necessary for the assembly of the functional NOX2 protein (Lam *et al*. 2010). In Arabidopsis the ROP (RHO of plants) GTPase ROP2 is required for ROS formation in root hairs (Jones *et al.* 2007). Another possible activation/regulation pathway involves Ca^{2+}. In Arabidopsis, it was demonstrated that NADPH oxidase activity leads to higher amounts of cytoplasmic Ca^{2+} which in turn has a positive effect on their activity mediated through EF hands (Kimura *et al.* 2012). Similarly, a trichoblast-specific signal might activate the RTH5 protein through a small GTPase or calcium-dependent protein kinase (CDPK) to facilitate trichoblast differentiation (Figure 6B). It is likely that RTH5 is also regulated by and/or participates in feedback loops involving these factors.

As a first step towards the elucidation of the RTH5-dependent molecular networks in young maize roots, a comparative RNA-Seq analysis was performed on 6-day-old wild-type versus *rth5* primary roots. Consistent with the suggested function of RTH5 only two major biological functions were overrepresented among the differentially expressed genes in a gene ontology (GO) enrichment analysis. First, the GO term “oxidation/reduction” was enriched. Genes in this class included four members of the *rboh* gene family, including *rth5* as discussed above. Moreover, this class also contains many genes related to oxidative stress including several peroxidases. As discussed above these peroxidases act downstream of RTH5 and facilitate the loosening of the elongating root hairs. This function connects the “oxidation/reduction” GO class with the GO subgroup “cellulose biosynthesis”. Cellulose is the most abundant plant polysaccharide (Carpita and McCann 2001) and biopolymer *per se*. Cellulose biosynthesis is a crucial step in root hair elongation that follows peroxidase mediated cell wall loosening (Figure 6A). In Arabidopsis it has been demonstrated that mutations in cellulose biosynthesis genes can result in defective tip growth and aberrant elongation of root hairs (Wang *et al*., 2001; Favery *et al*., 2001; Park *et al*., 2013). In summary, both overrepresented GO terms “oxidation/reduction” and “carbohydrate biosynthesis” are directly connected to maize root hair formation. Future reverse genetic analyses of candidate genes identified in this RNA-Seq analysis may therefore help to better define the genetic control of maize root hair formation.

Experimental procedures

Plant material and growth conditions

The mutation was initially induced by EMS (Ethyl methanesulfonate) mutagenesis of the Pioneer inbred line 114748/AD. Mutants used in the present study were progeny of plants backcrossed 10 times to the inbred line B73 (Schnable laboratory stock 00g-1542-1).
Kernels were surface sterilized as described previously (Nestler *et al.* 2011) and germinated in moist paper rolls at a 16 h light, 8 h dark cycle at 26 °C in distilled water.

Binocular imaging and environmental scanning electron microscopy

A Zeiss Stemi SV8 Binocular (www.zeiss.com) coupled with a Powershot G2 camera (www.canon.de) was used to document root hairs at a 20x magnification. Root hair length was determined via WinRhizo Software (www.regent.qc.ca). A Philips XL30 FEI environmental scanning electron microscope (eSEM; www.philips.de) was used for surface illustration of fresh four-day-old primary roots without fixation or tissue drying.

Bulked segregant analysis (BSA)

Sequenom-based BSA (bulked segregant analysis) (Liu *et al*. 2010) was used to map the *rth5* gene. 89 individuals from an F_2-family were phenotypically divided into two bulks: mutant and non-mutant. Equal quantities of root tissue were pooled from each individual in each bulk. DNA was extracted from the two tissue bulks and then subjected to Sequenom-based SNPtyping using ~1,000 SNP markers.

Fine-scale mapping of *rth5*

Multiple markers located on the long arm of chromosome 3 were used to genotype 80 *rth5* mutant individuals from an F_2-population (Table S1). An *rth5* mutant individual in a B73 genetic background was crossed with the Mo17 inbred line and the resulting F_1-seeds were backcrossed to Mo17 to create an F_1BC population. Two SNP (single nucleotide polymorphism) markers, SNP2673 and SNP6262, were used to genotype 512 F_1BC individuals. In total, 65 recombinants were identified between SNP2673 and SNP6262, each of which was self-pollinated. The root hair phenotypes of self-pollinated progeny were scored to infer whether or

not specific F_1BC_1 recombinants carried the *rth5* mutant allele. In parallel, the recombinants were genotyped with a series of molecular markers (Figure 2A). Based on an analysis of the resulting genotyping and phenotyping data, the *rth5* mutant was mapped to the 179.9-182.3 Mb interval of chromosome 3 in AGPv1. To further narrow down the *rth5* interval, a larger F_1BC population (N=~5,000) was genotyped with SNP markers SNP90373 and M_109352. In total, 440 recombinants between these two marker loci were identified and genotyped for *rth5* as described above. After genotyping all available recombinants (65 + 440) with 35 SNP markers (15 of which are co-dominant in this population) the *rth5* gene was mapped to the interval 180.1-180.4 Mb.

Identification of independent *rth5* mutant alleles

Three independent alleles, *rth5-2*, *rth5-3, and rth5-4*, were identified by a reverse genetic screen of *Mutator* stocks at Pioneer Hi-Bred. Confirmation of the candidate seedlings displaying a roothairless phenotype was performed by PCR mapping of the *Mutator* insertion with a general *Mutator* (Mu) oligonucleotide primer (Dietrich *et al.* 2002) and an *rth5*-specific oligonucleotide primer (5'-GCACATCTCCCGGATAAATTG-3'). The amplification product contained 39 bp beyond the Mu TIR sequence sufficient to identify the *Mutator* element (Dietrich *et al*. 2002). *Mu* insertions were found in positions 1300, 1931, and 1968 bp of the genomic *rth5* sequence counting from the ATG start codon in the alleles *rth5-2*, *rth5-3*, and *rth5-4*, respectively.

RTH5 protein domain prediction

Several bioinformatic tools were used to predict protein domains: InterProScan (www.ebi.ac.uk/Tools/pfa/iprscan), MyHits (myhits.isb-sib.ch), SMART (smart.embl-heidelberg.de) and TMHMM (www.cbs.dtu.dk/services/TMHMM). Domains predicted by at least two search tools were summarized in the protein domain structure (Figure 2B).

Phylogenetic analyses

The protein sequences of RTH5 homologs were obtained by blasting the RTH5 sequence against species-specific databases at maizesequence.org, rice.plantbiology.msu.edu, soybean.org, and TAIR.org. The DNA Baser software (dnabaser.com) was used to combine all sequences into a Fasta file which was used for alignment and calculation of a phylogenetic tree

by MEGA4.0 (Tamura *et al.* 2007) using the Neighbor joining algorithm (Bootstrap, 1000 replications).

RNA *in situ* hybridization

Primary roots of three-day-old seedlings were fixed and embedded in paraffin as described previously (Hochholdinger *et al.* 2008). The RNA probe for hybridization was generated by amplification of 282 bp from the 3´-end of the *rth5* gene with the oligonucleotide primers forward 5'-GTGTACCCGAAGATCCGATG-3', and reverse 5'-GACAGCTCGGGCAGAAAGAC-3'. The amplicon was cloned into the pGEM T-easy vector (Promega, www.promega.com) in sense and antisense directions. *In vitro* transcription of the probes and digoxigenin-labeling was performed using the SP6 polymerase (NEB, www.neb.com/nebecomm/default.asp) according to the manufacturer's protocol. RNA *in situ* hybridization was performed according to (Jackson 1992). A Zeiss Axioplan 2 microscope (www.zeiss.com) in combination with a Photometrics Cool Snapcamera (Roper Scientific GmbH, www.roperscientific.com) was used for image acquisition.

Quantitative RT-PCR

For qRT-PCR, RNA was extracted from approximately 100 mg of different maize tissues with the RNeasy Plant Mini Kit (Qiagen, www.qiagen.com) according to the manufacturer's protocol, including on-column DNase I digestion (Fermentas, www.fermentas.de). Isolation and harvesting of root hairs was performed as described previously (Nestler, *et al.* 2011). cDNA was prepared from 500 ng total RNA by using the qScript cDNA Super Mix (Quanta BioSciences, www.quantabio.com). qRT-PCR experiments were performed using MESA Green or Blue qPCR Mastermix Plus for SYBR Assay no ROX kit (Eurogentec, www.eurogentec.com). All experiments were conducted in three biological replicates and three technical replicates per biological replicate in a CFX384 Real-Time PCR Detection System (Bio-Rad, www.bio-rad.com). The efficiency for every oligonucleotide primer pair (summarized in Table S7) was determined by a dilution series. Expression was calculated relative to the reference gene *myosin* (GenBank AC486090G09.x1), which has previously been used as expression standard in maize root assays (Dembinsky *et al.* 2007).

Antibody preparation and immune histochemistry

A polyclonal antibody was produced by incubating rabbits with a specific RTH5 peptide with the amino acid sequence VAGMRPGRMTRMQSSAQM.

Sample preparation was slightly modified from the RNA *in situ* hybridization protocol. Fixation was performed using 4% formamide solution. After sectioning, the samples were deparaffined using RotiClear (Roth, www.carl-roth.de) and rehydrated using decreasing ethanol concentrations (90%, 50%, 25%) in Microtubules stabilizing buffer (MtSB) (Albertini *et al.* 1984). Unspecific binding was blocked by 3% BSA in 1x MtSB, followed by incubation with the RTH5 antibody (1:100 in 1x MtSB) overnight at 4 °C. After six washing steps in 1x MtSB the samples were incubated for 2 h with the secondary antibody ZytoChem Plus AP Polymer anti-Rabbit (ZytoMed, www.zytomed-systems.de) according to the manufacturer's protocol. After washing with a buffer containing 100 mM Tris, 100 mM NaCl, and 50 mM $MgCl_2$, the signal was detected using the Roche NBT/BCIP stock solution (www.roche.de) by incubation in the dark for 5-10 min. The reaction was stopped by three water incubations. Images were obtained as described for RNA *in situ* hybridization experiments.

Detection of superoxide and hydrogen peroxide

Superoxide was detected by incubating root samples in 0.5 mM Nitro blue tetrazolium chloride (NBT) in 0.1 M KCl/ 0.1 M NaCl solution which forms an insoluble blue formazan precipitate upon reaction with superoxide (Bielski *et al.* 1980). To detect hydrogen peroxide two dyes were used: DAB (3,3-diaminobenzidine) and 2,7-dichlorodihydrofluorescein diacetate (H_2DCF-DA). DAB forms a brown precipitate when oxidized by peroxidase activity (Thordal-Christensen *et al*. 1997). Seedlings were incubated overnight in 1mg/ml DAB dissolved in water. H_2DCF-DA emits a green fluorescence that corresponds to cytoplasmic H_2O_2 levels (Keston and Brandt 1965). The stock solution was prepared by dissolving 1 mg H_2DCF-DA in 1 ml DMSO, and mixing with 1 ml H_2O. To obtain the working solution a dilution in 200 ml H_2O was prepared.

Three-day-old seedlings were incubated for 45 min in the dark in petri dishes, each of which contained a detection solution. The signal was detected by mounting primary roots in water on a microscopic slide covered by a 60 mm cover slip. Excitation of H_2DCF-DA was performed at 488 nm. Emission was detected at 525 nm using a Zeiss Axioplan 2 microscope (www.zeiss.com).

RNA-Seq experiment

Seeds from an F_2-family segregating for *rth5* after nine generations of backcrossing to the inbred B73 were grown as described above. 3 cm root tips were collected from 6-day-old *rth5* mutants and wild-type siblings. Two mutant and two wild-type pools were collected. Each pool consisted of root tissues from six individuals. From each pool RNA was extracted using RNeasy mini kits (Qiagen) with DNase I treatment following the manufacturer's protocol. RNA quality was analyzed using a Bioanalyer 2100 RNA Nano chip. RNA-Seq libraries were constructed using an Illumina RNA-Seq sample preparation kit following the manufacturer's protocol. The four libraries were sequenced on an Illumina HiSeq2000 at the Iowa State University DNA facility, generating 99 bp single-end reads and deposited at GenBank (accession no. SRP020528).

Trimming and mapping of RNA-Seq reads

Raw reads were subjected to quality checking and trimming to remove low quality bases using a custom trimming pipeline (Liu *et al*. 2012). Trimmed reads were aligned to the B73 reference genome (ZmB73_RefGen_v2) using GSNAP (Wu and Nacu 2010), allowing ≤2 mismatches every 50 bp and 2 bp tails per 50 bp. Only uniquely mapped reads were used for subsequent analyses. The read depth of each gene in the filtered gene set (ZmB73_FGSv2; http://ftp.maizesequence.org/current/filtered-set/, Release 5b.60) was computed based on the coordinates of mapped reads and the annotated locations of genes in the B73 reference genome.

Differential expression analysis of RNA-Seq

Genes with ≥20 RNA-Seq reads across all four biological replicates were tested for differential expression between the *rth5* mutant and wild-type using the R package *QuasiSeq* (http://cran.r-project.org/web/packages/QuasiSeq). The negative binomial *QLSpline* method implemented in the *QuasiSeq* package was used to compute a *p*-value for each gene. The 0.75 quantile of reads from each sample was used as the normalization factor (Bullard *et al.* 2010). An approach for controlling for multiple testing (Benjamini *et al*. 1995) was used to convert *p*-values to *q*-values. To approximately control the false discovery rate (FDR) at 5%, only genes with *q*-values <0.05 were declared to be differentially expressed.

Gene ontology (GO) enrichment analysis of significantly differentially expressed genes

The Gene Ontology (GO) of specific genes and the overrepresentation of GO terms were conducted using the single enrichment analysis of the AgriGo platform (http://bioinfo.cau.edu.cn/agriGO/analysis.php).

Acknowledgement

We thank Lisa Coffey (Iowa State University) for maintaining genetic stocks and conducting genetic crosses and Knut Wichterich (University of Bonn) for his support in generating the eSEM images of primary roots. We thank Mitzi J. Wilkening at the Genomic Technologies Facility at Iowa State University for conducting the Sequenom-based Bulk Segregation Analysis (BSA) experiment. This project was funded by the Deutsche Forschungsgemeinschaft (DFG) project HO2249/9 to F.H.

Supporting information

Figure S1. Phenotype of *roothairless 5* in different root types.

Binocular pictures of ten-day-old wild-type (**a**-**d**) and *rth5* mutant (**e**-**g**) primary (**a**, **e**), seminal (**b**, **f**), crown (**c**, **g**) and lateral roots (**d**, **h**). Scale bar 500 µm. Root hair length was determined using WinRhizo software (**I**, n=12). *P*-values obtained via Student's t-test, *p*-value ***: ≤0.001. Error bars represent standard deviation.

Figure S2: **Alignment of RTH5 and its homologs from maize, soybean, rice and Arabidopsis.**

Proteins are listed according to their order in the phylogenetic tree (Figure 3). Sequences were aggregated in units of ten amino acids (aa). Five and more aa per unit are depicted as boxes, <5 as lines. Color code: red - conserved in both groups, blue - conserved in group I, green - conserved in group II, dark gray - annotated functional domain, light gray - no functional annotation.

Figure S3: Expression analysis of maize *rboh* genes.

Quantitative RT-PCR analysis of different root tissues of all maize *rboh* gene family members in 3-day-old B73 seedlings. Coleoptilar nodes and leaves were harvested from 7-day-old seedlings. Expression was calculated (n=3) relative to the reference gene *myosin* (Genbank AC: 48090G09.x1). Error bars represent standard deviations. Please note the different relative expression levels on the y-axes of the different genes have been adjusted to highlight tissue-specific expression differences for individual genes.

Figure S4. Expression of *rth5* in various tissues.

Expression of the *rth5* gene in various tissues was illustrated in normalized FPKM (fragments per kilobase of exon per million of fragments mapped) values. The data was downloaded from qteller.com as of 4/1/2013.

Figure S5. *Rth5* transcript and RTH5 protein abundance in wild-type and *rth5* mutants.

(**a**) Expression of *rth5* in 3-day-old wild-type and *rth5* mutant primary roots. Quantitative RT-PCR levels relative to the *myosin* gene (Genbank AC: 48090G09.x1). Error bars indicate standard deviation of four biological replicates. (**b**) Detection of RTH5 protein via Western blot experiments in three biological replicates. (**c**) Immunohistochemistry on paraffin-embedded cross sections of the differentiation zone (top row, scale bars 50 µm) and longitudinal sections (scale bars 100 µm) of elongation zone (middle) and differentiation zone (lower lane). Arrows indicate root hairs.

Figure S6. RNA-Seq analysis of *rth5* versus wild-type primary roots

(**a**) Histogram of *p*-values resulting from differential expression analyses. QuasiSeq was used to test the null hypothesis that expression of a given gene is not different between the two genotypes. A *p*-value was obtained for each informative gene. The distribution of *p*-values under the null hypothesis (no differentially expressed genes exist) is a uniform distribution in the range of 0-1. (**b**) MA-similar plot from RNA-Seq experiments. MA-similar plot providing an overview of the correlation of gene expression changes versus expression intensity by plotting the $\log_2$ of the fold change of *rth5*/wild-type (y-axis) against the $\log_2$ of the mean of gene expression in *rth5* and wild-type (x-axis). Each dot represents an expressed gene. Significantly differentially expressed genes are highlighted in red. (**c**) Volcano plot displaying differential gene

expression patterns between *rth5* and wild-type. The y-axis denotes negative $\log_{10}$ *p*-values of each expressed gene. The x-axis denotes $\log_2$ fold changes of *rth5*/wild-type. Each dot represents an expressed gene. Red dots denote down-regulated genes in *rth5*, blue dots denote up-regulated genes in *rth5*. The horizontal dash line indicates the 5% FDR cutoff.

Table S1. Summary of markers used in the fine-mapping experiment.

Table S2. Summary of RNA-Seq mapping.

Table S3. Summary of reads per gene and replicate and statistical analysis of differential expression between *rth5* mutants and wild-type roots.

Table S4. Gene ontology terms related to biological functions that are overrepresented among the differentially expressed genes.

Table S5. Relation of genes included in the GO term oxidation/reduction and its subgroups.

Table S6. Relation of genes included in the GO term carbohydrate metabolic process and its subgroups.

Table S7. Oligonucleotide primers used for qRT-PCR experiments.

References

Albertini, D.F., Herman, B. and Sherline, P. (1984) *In vivo* and *in vitro* studies on the role of HMW-MAPs in taxol-induced microtubule bundling. *Eur J Cell Biol*, **33**, 134-143.

Bedard, K., Lardy, B. and Krause, K.H. (2007) NOX family NADPH oxidases: not just in mammals. *Biochimie*, **89**, 1107-1112.

Benjamini, Y. and Hochberg, Y. (1995) Controlling the false discovery rate: a practical and powerful approach to multiple testing. *J. Roy. Statistical Society, Series B*, **57**, 289–300.

Bensen, R.J., Johal, G.S., Crane, V.C., Tossberg, J.T., Schnable, P.S., Meeley, R.B., Briggs, S.P. (1995) Cloning and Characterization of the Maize *An1* Gene. *The Plant Cell*, 7, 75-84.

Bibikova, T.N., Jacob, T., Dahse, I. and Gilroy, S. (1998) Localized changes in apoplastic and cytoplasmic pH are associated with root hair development in *Arabidopsis thaliana*. *Development*, **125**, 2925-2934.

Bielski, B.H.J., Shiue, G.G. and Bajuk, S. (1980) Reduction of Nitro Blue Tetrazolium by Co_2^- and O^-_2- Radicals. *J Phys Chem-Us*, **84**, 830-833.

Bruex, A., Kainkaryam, R.M., Wieckowski, Y., Kang, Y.H., Bernhardt, C., Xia, Y., Zheng, X., Wang, J.Y., Lee, M.M., Benfey, P., Woolf, P.J. and Schiefelbein, J. (2012) A gene regulatory network for root epidermis cell differentiation in *Arabidopsis*. *PLoS Genet*, **8**, e1002446.

Bullard, J.H., Purdom, E., Hansen, K.D. and Dudoit, S. (2010) Evaluation of statistical methods for normalization and differential expression in mRNA-Seq experiments. *BMC Bioinformatics*, **11**, 94.

Carpita, N. and McCann, M. (2000) The cell wall. In B Buchanan, W Gruissem, R Jones, eds, Biochemistry and Molecular Biology of Plants. American Society of Plant Physiologists, Rockville, MD.

Clowes, F.A.L. (2000) Pattern in root meristem development in angiosperms. *New Phytologist*, **146**, 83-94.

Cormack, R.G.H. (1947) A Comparative Study of Developing Epidermal Cells in White Mustard and Tomato Roots. *Am. J. Bot.*, **34**, 310-314.

Dembinsky, D., Woll, K., Saleem, M., Liu, Y., Fu, Y., Borsuk, L.A., Lamkemeyer, T., Fladerer, C., Madlung, J., Barbazuk, B., Nordheim, A., Nettleton, D., Schnable, P.S. and Hochholdinger, F. (2007) Transcriptomic and proteomic analyses of pericycle cells of the maize primary root. *Plant Physiol.*, **145**, 575-588.

Dietrich, C.R., Cui, F., Packila, M.L., Li, J., Ashlock, D.A., Nikolau, B.J. and Schnable, P.S. (2002) Maize *Mu* transposons are targeted to the 5' untranslated region of the *gl8* gene and sequences flanking *Mu* target-site duplications exhibit nonrandom nucleotide composition throughout the genome. *Genetics*, **160**, 697-716.

Dolan, L. (2001) How and where to build a root hair. *Curr. Opin. Plant Biol.*, **4**, 550-554.

Dolan, L., Duckett, C.M., Grierson, C., Linstead, P., Schneider, K., Lawson, E., Dean, C., Poethig, S. and Roberts, K. (1994) Clonal Relationships and Cell Patterning in the Root Epidermis of *Arabidopsis*. *Development*, **120**, 2465-2474.

Favery, B., Ryan, E., Foreman, J., Linstead, P., Boudonck, K., Steer, M., Shaw, P. and Dolan, L. (2001) KOJAK encodes a cellulose synthase-like protein required for root hair cell morphogenesis in Arabidopsis. *Genes Dev.*, **15**, 79-89.

Foreman, J., Demidchik, V., Bothwell, J.H.F., Mylona, P., Miedema, H., Torres, M.A., Linstead, P., Costa, S., Brownlee, C., Jones, J.D.G., Davies, J.M. and Dolan, L. (2003) Reactive oxygen species produced by NADPH oxidase regulate plant cell growth. *Nature*, **422**, 442-446.

Fry, S.C. (1998) Oxidative scission of plant cell wall polysaccharides by ascorbate-induced hydroxyl radicals. *Biochem J*, **332 (Pt 2)**, 507-515.

Galletti, R., Denoux, C., Gambetta, S., Dewdney, J., Ausubel, F.M., De Lorenzo, G. and Ferrari, S. (2008) The AtrbohD-mediated oxidative burst elicited by oligogalacturonides in *Arabidopsis* is dispensable for the activation of defense responses effective against *Botrytis cinerea*. *Plant Physiol.*, **148**, 1695-1706.

Gapper, C. and Dolan, L. (2006) Control of plant development by reactive oxygen species. *Plant Physiol.*, **141**, 341-345.

Gilroy, S. and Jones, D.L. (2000) Through form to function: root hair development and nutrient uptake. *Trends Plant Sci*, **5**, 56-60.

Greene, E.A., Codomo, C.A., Taylor, N.E., Henikoff, J.G., Till, B.J., Reynolds, S.H., Enns, L.C., Burtner, C., Johnson, J.E., Odden, A.R., Comai, L. and Henikoff, S. (2003) Spectrum of chemically induced mutations from a large-scale reverse-genetic screen in *Arabidopsis*. *Genetics*, **164**, 731-740.

Hochholdinger, F. and Feix, G. (1998) Early post-embryonic root formation is specifically affected in the maize mutant *lrt1*. *Plant J*, **16**, 247-255.

Hochholdinger, F. and Nestler, J. (2012) Genetics and Genomics of Plant Root Development. *Encyclopedia of Genetics*, **in press**.

Hochholdinger, F., Wen, T.J., Zimmermann, R., Chimot-Marolle, P., Silva, O.D.E., Bruce, W., Lamkey, K.R., Wienand, U. and Schnable, P.S. (2008) The maize (*Zea mays* L.) *roothairless3* gene encodes a putative GPI-anchored, monocot-specific, COBRA-like protein that significantly affects grain yield. *Plant J.*, **54**, 888-898.

Ishida, T., Kurata, T., Okada, K. and Wada, T. (2008) A genetic regulatory network in the development of trichomes and root hairs. *Annu. Rev. Plant Biol.*, **59**, 365-386.

Ivanov, R., Brumbarova, T. and Bauer, P. (2012) Fitting into the harsh reality: regulation of iron-deficiency responses in dicotyledonous plants. *Mol Plant*, **5**, 27-42.

Jackson, D. (1992) *In situ* hybridization in plants. *Mol. Plant Pathol.*, **Oxford**, 163-174.

Jones, M.A., Raymond, M.J., Yang, Z. and Smirnoff, N. (2007) NADPH oxidase-dependent reactive oxygen species formation required for root hair growth depends on ROP GTPase. *J Exp Bot*, **58**, 1261-1270.

Kawahara, T., Quinn, M.T. and Lambeth, J.D. (2007) Molecular evolution of the reactive oxygen-generating NADPH oxidase (Nox/Duox) family of enzymes. *BMC Evol Biol*, **7**, 109.

Keston, A.S. and Brandt, R. (1965) Fluorometric Analysis of Ultramicro Quantities of Hydrogen Peroxide. *Anal. Biochem.*, **11**, 1-&.

Kimura, S., Kaya, H., Kawarazaki, T., Hiraoka, G., Senzaki, E., Michikawa, M. and Kuchitsu, K. (2012) Protein phosphorylation is a prerequisite for the Ca^{2+}-dependent activation of *Arabidopsis* NADPH oxidases and may function as a trigger for the positive feedback regulation of Ca^{2+} and reactive oxygen species. *Biochim Biophys Acta*, **1823**, 398-405.

Kwak, J.M., Mori, I.C., Pei, Z.M., Leonhardt, N., Torres, M.A., Dangl, J.L., Bloom, R.E., Bodde, S., Jones, J.D. and Schroeder, J.I. (2003) NADPH oxidase *AtrbohD* and *AtrbohF* genes function in ROS-dependent ABA signaling in *Arabidopsis*. *EMBO J*, **22**, 2623-2633.

Lam, G.Y., Huang, J. and Brumell, J.H. (2010) The many roles of NOX2 NADPH oxidase-derived ROS in immunity. *Seminars in immunopathology*, **32**, 415-430.

Lee, M.M. and Schiefelbein, J. (1999) WEREWOLF, a MYB-related protein in *Arabidopsis*, is a position-dependent regulator of epidermal cell patterning. *Cell*, **99**, 473-483.

Lid, S.E., Al, R.H., Krekling, T., Meeley, R.B., Ranch, J., Opsahl-Ferstad, H.G. and Olsen, O.A. (2004) The maize *disorganized aleurone layer 1* and *2* (*dil1*, *dil2*) mutants lack control of the mitotic division plane in the aleurone layer of developing endosperm. *Planta*, **218**, 370-378.

Lin, F., Ding, H., Wang, J., Zhang, H., Zhang, A., Zhang, Y., Tan, M., Dong, W. and Jiang, M. (2009) Positive feedback regulation of maize NADPH oxidase by mitogen-activated protein kinase cascade in abscisic acid signalling. *J Exp Bot*, **60**, 3221-3238.

Liszkay, A., Kenk, B. and Schopfer, P. (2003) Evidence for the involvement of cell wall peroxidase in the generation of hydroxyl radicals mediating extension growth. *Planta*, **217**, 658-667.

Liszkay, A., van der Zalm, E. and Schopfer, P. (2004) Production of reactive oxygen intermediates $O^{-}_{2}{}^{\cdot}$, H_2O_2, and $OH^{\cdot}$ by maize roots and their role in wall loosening and elongation growth. *Plant Physiol.*, **136**, 3114-3123.

Liu, S., Chen, H.D., Makarevitch, I., Shirmer, R., Emrich, S.J., Dietrich, C.R., Barbazuk, W.B., Springer, N.M. and Schnable, P.S. (2010) High-throughput genetic mapping of mutants via quantitative single nucleotide polymorphism typing. *Genetics*, **184**, 19-26.

Liu, S., Yeh, C.-T., Tang, H.M., Nettleton, D. and Schnable, P.S. (2012) Gene Mapping via Bulked Segregant RNA-Seq (BSR-Seq). *PLoS ONE*, **7**, e36406.

Livanos, P., Galatis, B., Quader, H. and Apostolakos, P. (2012) Disturbance of reactive oxygen species homeostasis induces atypical tubulin polymer formation and affects mitosis in root-tip cells of *Triticum turgidum* and *Arabidopsis thaliana*. *Cytoskeleton (Hoboken)*, **69**, 1-21.

Masucci, J.D., Rerie, W.G., Foreman, D.R., Zhang, M., Galway, M.E., Marks, M.D. and Schiefelbein, J.W. (1996) The homeobox gene *GLABRA 2* is required for position-dependent cell differentiation in the root epidermis of *Arabidopsis thaliana*. *Development*, **122**, 1253-1260.

Nauseef, W.M. (2008) Biological roles for the NOX family NADPH oxidases. *J Biol Chem*, **283**, 16961-16965.

Nestler, J., Schutz, W. and Hochholdinger, F. (2011) Conserved and unique features of the maize (*Zea mays* L.) root hair proteome. *J Proteome Res*, **10**, 2525-2537.

Park, S., Szumlanski, A.L., Gu, F., Guo, F. and Nielsen, E. (2011) A role for CSLD3 during cell-wall synthesis in apical plasma membranes of tip-growing root-hair cells. *Nat. Cell. Biol.*, **13**, 973-980.

Parker, J.S., Cavell, A.C., Dolan, L., Roberts, K. and Grierson, C.S. (2000) Genetic interactions during root hair morphogenesis in *Arabidopsis*. *Plant Cell*, **12**, 1961-1974.

Schiefelbein, J.W. and Somerville, C. (1990) Genetic control of root hair development in *Arabidopsis thaliana*. *Plant Cell*, **2**, 235-243.

Takeda, S., Gapper, C., Kaya, H., Bell, E., Kuchitsu, K. and Dolan, L. (2008) Local positive feedback regulation determines cell shape in root hair cells. *Science*, **319**, 1241-1244.

Tamura, K., Dudley, J., Nei, M. and Kumar, S. (2007) MEGA4: Molecular Evolutionary Genetics Analysis (MEGA) software version 4.0. *Mol Biol Evol*, **24**, 1596-1599.

Thordal-Christensen, H., Zhang, Z., Wei, Y., Collinge, D.B. (1997) Subcellular localization of H_2O_2 in plants. H_2O_2 accumulated in papillae and hypersensitive response during barley-powdery mildew interaction. *Plant J*, 11, 1187-1194.

Torres, M.A., Onouchi, H., Hamada, S., Machida, C., Hammond-Kosack, K.E. and Jones, J.D. (1998) Six *Arabidopsis thaliana* homologues of the human respiratory burst oxidase ($gp91^{phox}$). *Plant J*, **14**, 365-370.

Wada, T., Kurata, T., Tominaga, R., Koshino-Kimura, Y., Tachibana, T., Goto, K., Marks, M.D., Shimura, Y. and Okada, K. (2002) Role of a positive regulator of root hair development, CAPRICE, in *Arabidopsis* root epidermal cell differentiation. *Development*, **129**, 5409-5419.

Wang, X., Cnops, G., Vanderhaeghen, R., De Block, S., Van Montagu, M. and Van Lijsebettens, M. (2001) AtCSLD3, a cellulose synthase-like gene important for root hair growth in arabidopsis. *Plant Physiol.*, **126**, 575-586.

Wen, T.J., Hochholdinger, F., Sauer, M., Bruce, W. and Schnable, P.S. (2005) The *roothairless1* gene of maize encodes a homolog of *sec3*, which is involved in polar exocytosis. *Plant Physiol.*, **138**, 1637-1643.

Wen, T.J. and Schnable, P.S. (1994) Analyses of mutants of 3 genes that influence root hair development in *Zea mays* (Gramineae) suggest that root hairs are dispensable. *Am. J. Bot.*, **81**, 833-842.

Wi, S.J., Ji, N.R. and Park, K.Y. (2012) Synergistic biosynthesis of biphasic ethylene and reactive oxygen species in response to hemibiotrophic *Phytophthora parasitica* in tobacco plants. *Plant Physiol.*, **159**, 251-265.

Woll, K., Borsuk, L.A., Stransky, H., Nettleton, D., Schnable, P.S. and Hochholdinger, F. (2005) Isolation, characterization, and pericycle-specific transcriptome analyses of the novel maize lateral and seminal root initiation mutant *rum1*. *Plant Physiol.*, **139**, 1255-1267.

Wong, H.L., Pinontoan, R., Hayashi, K., Tabata, R., Yaeno, T., Hasegawa, K., Kojima, C., Yoshioka, H., Iba, K., Kawasaki, T. and Shimamoto, K. (2007) Regulation of rice NADPH oxidase by binding of Rac GTPase to its N-terminal extension. *Plant Cell*, **19**, 4022-4034.

Wu, T.D. and Nacu, S. (2010) Fast and SNP-tolerant detection of complex variants and splicing in short reads. *Bioinformatics*, **26**, 873-881.

Wymer, C.L., Bibikova, T.N. and Gilroy, S. (1997) Cytoplasmic free calcium distributions during the development of root hairs of *Arabidopsis thaliana*. *Plant J.*, **12**, 427-439.

Yamauchi, T., Rajhi, I. and Nakazono, M. (2011) Lysigenous aerenchyma formation in maize root is confined to cortical cells by regulation of genes related to generation and scavenging of reactive oxygen species. *Plant Signal Behav*, **6**, 759-761.

Yi, S.Y., Lee, D.J., Yeom, S.I., Yoon, J., Kim, Y.H., Kwon, S.Y. and Choi, D. (2010) A novel pepper (*Capsicum annuum*) receptor-like kinase functions as a negative regulator of plant cell death via accumulation of superoxide anions. *New Phytol*, **185**, 701-715.

Zhang, A., Zhang, J., Ye, N., Cao, J., Tan, M. and Jiang, M. (2010) ZmMPK5 is required for the NADPH oxidase-mediated self-propagation of apoplastic H_2O_2 in brassinosteroid-induced antioxidant defence in leaves of maize. *J Exp Bot*, **61**, 4399-4411.

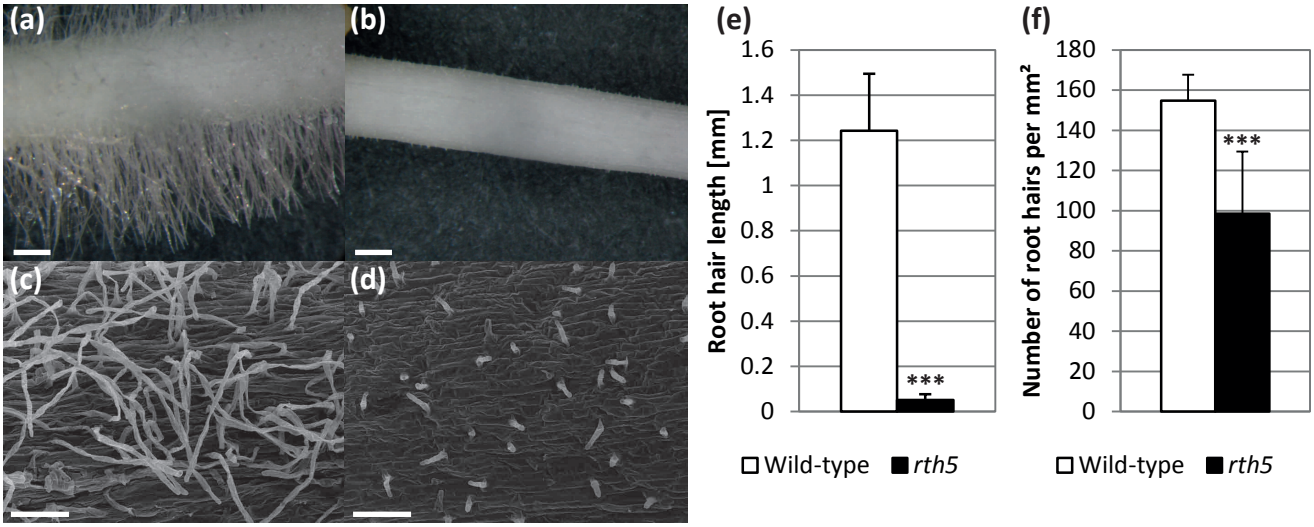

Figure 1. Phenotype of *roothairless5*.
Binocular and eSEM pictures of four-day-old wild-type (**a**, **c**) and *rth5* mutant (**b**, **d**) primary roots. (**e**) Root hair length (n=12). (**f**) Root hair density per mm² (n=3). *P*-values were obtained via Student's t-test, *p*-value ***: ≤0.001. Error bars indicate standard deviation. Scale bar (**a**, **b**) 500 µm, (**c**, **d**) 100 µm.

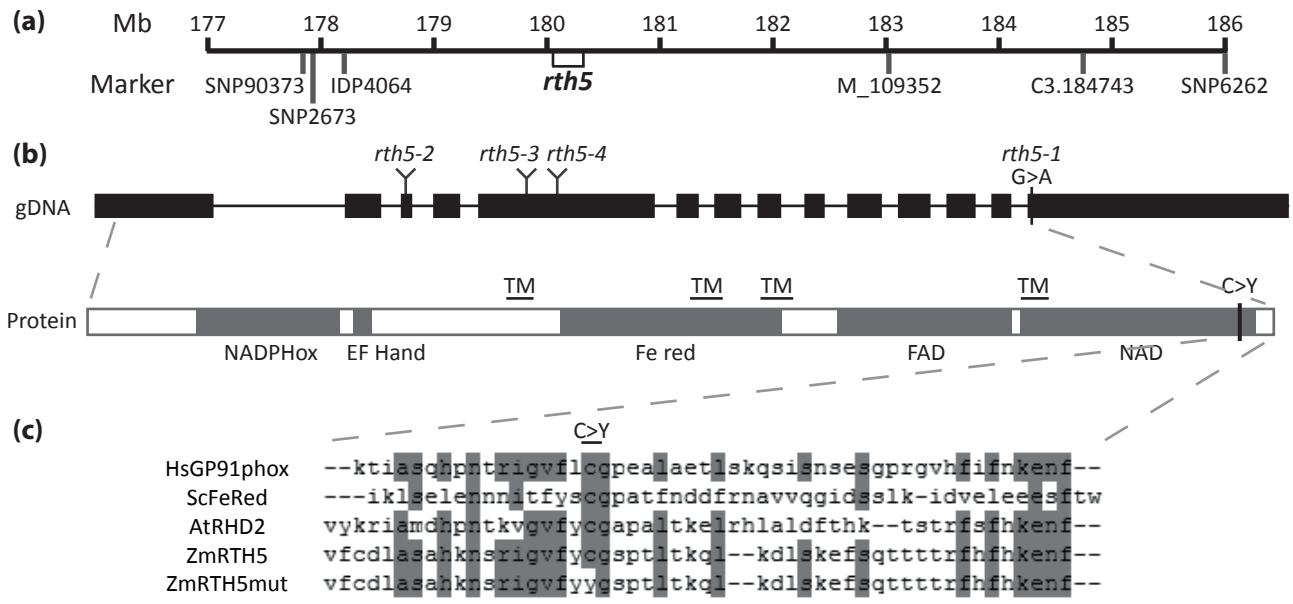

Figure 2. Mapping of *rth5*.
(**a**) Map-based cloning experiments positioned the *rth5* gene within a 280 kb interval of chromosome 3. (**b**) A G to A (G>A) substitution in the last exon of the candidate gene GRMZM2G426953 results in a cysteine by tyrosine (C>Y) substitution in the protein sequence of the *rth5-1* allele at position 821. The positions of *Mu* transposon insertions in three additional alleles, *rth5-2*, *rth5-3*, and *rth5-4* are indicated. (**c**) Alignment of the C-terminal 50 amino acids of human, yeast and Arabidopsis NADPH oxidases and wild-type and mutant RTH5. TM: trans-membrane, NADPHox: NADPH oxidase domain, EF hand: Ca^{2+} binding site, Fe red: Ferric reduction domain, FAD / NAD: FAD / NAD binding site, Hs: *Homo sapiens*, Sc: *Saccharomyces cerevisiae*, At: *Arabidopsis thaliana*, Zm: *Zea mays*.

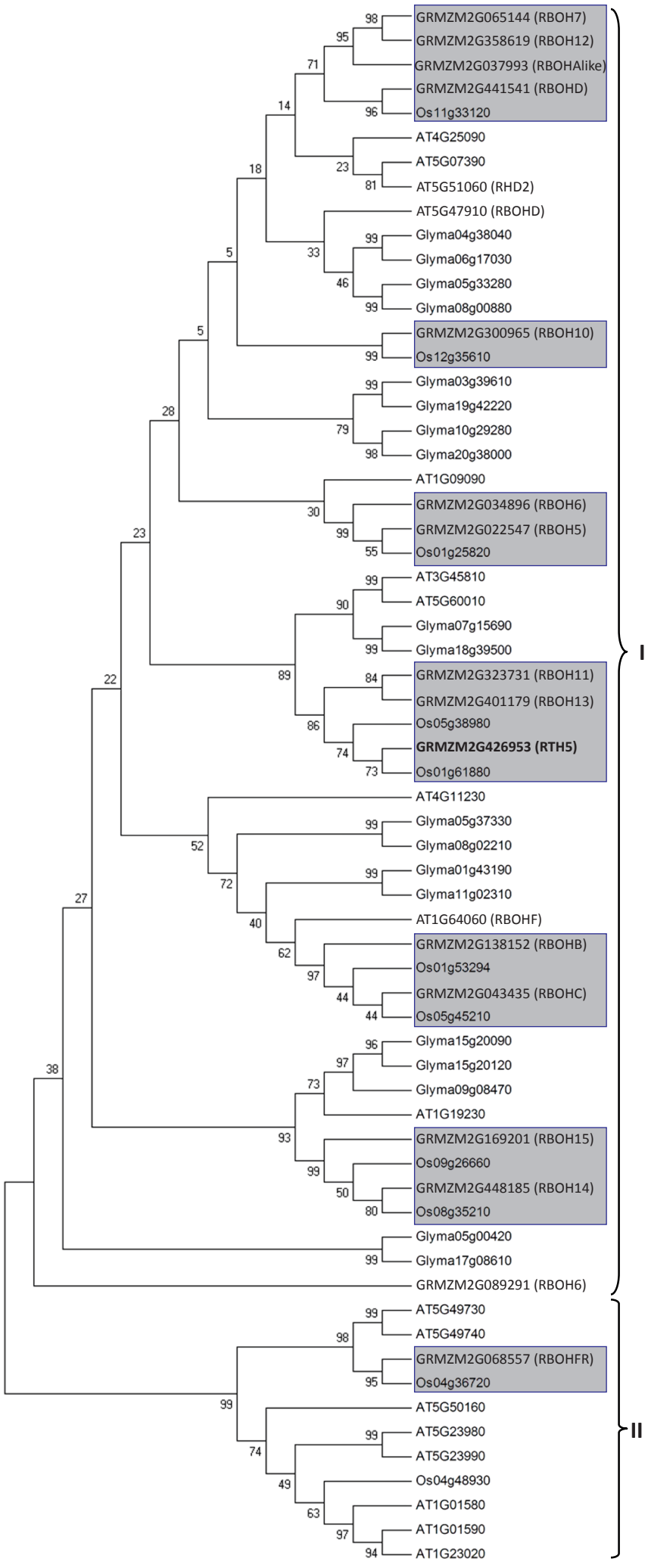
GRMZM2G065144 (RBOH7)
GRMZM2G358619 (RBOH12)
GRMZM2G037993 (RBOHAlike)
GRMZM2G441541 (RBOHD)
Os11g33120
AT4G25090
AT5G07390
AT5G51060 (RHD2)
AT5G47910 (RBOHD)
Glyma04g38040
Glyma06g17030
Glyma05g33280
Glyma08g00880
GRMZM2G300965 (RBOH10)
Os12g35610
Glyma03g39610
Glyma19g42220
Glyma10g29280
Glyma20g38000
AT1G09090
GRMZM2G034896 (RBOH6)
GRMZM2G022547 (RBOH5)
Os01g25820
AT3G45810
AT5G60010
Glyma07g15690
Glyma18g39500
GRMZM2G323731 (RBOH11)
GRMZM2G401179 (RBOH13)
Os05g38980
GRMZM2G426953 (RTH5)
Os01g61880
AT4G11230
Glyma05g37330
Glyma08g02210
Glyma01g43190
Glyma11g02310
AT1G64060 (RBOHF)
GRMZM2G138152 (RBOHB)
Os01g53294
GRMZM2G043435 (RBOHC)
Os05g45210
Glyma15g20090
Glyma15g20120
Glyma09g08470
AT1G19230
GRMZM2G169201 (RBOH15)
Os09g26660
GRMZM2G448185 (RBOH14)
Os08g35210
Glyma05g00420
Glyma17g08610
GRMZM2G089291 (RBOH6)
AT5G49730
AT5G49740
GRMZM2G068557 (RBOHFR)
Os04g36720
AT5G50160
AT5G23980
AT5G23990
Os04g48930
AT1G01580
AT1G01590
AT1G23020
I
II

Figure 3

Figure 3. Phylogenetic tree of NADPH oxidases of maize, rice, Arabidopsis and soybean.
Two subfamilies can be distinguished by the presence or absence of several conserved domains in group I and II (Figure S2). Monocot specific clades/ subclades are highlighted with gray boxes.

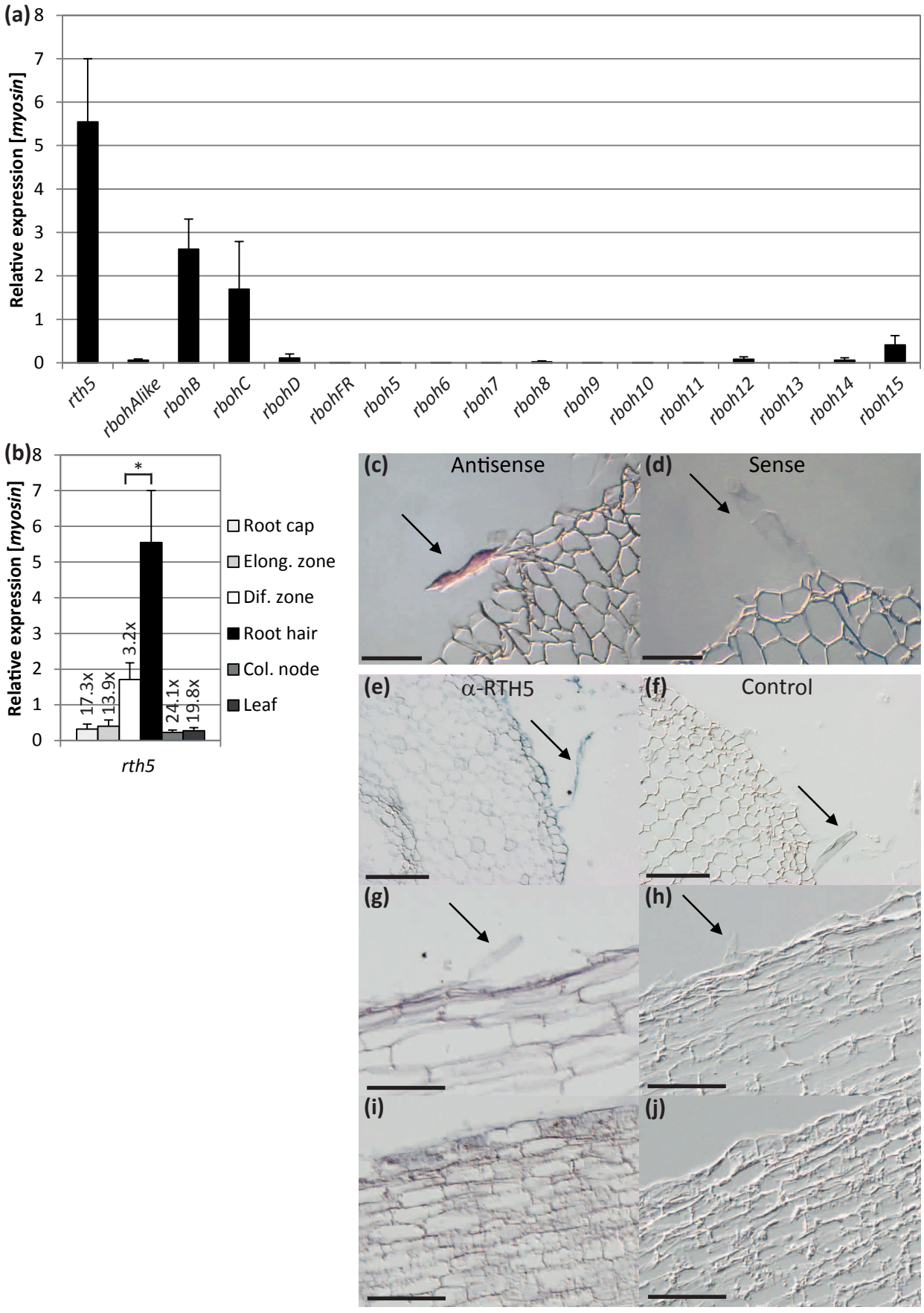

Figure 4. Tissue-specific expression of *rth5* transcripts and accumulation of RTH5 proteins.
(**a**) Expression of the *rth5* gene family members in root hairs by qPCR. (**b**) *rth5* expression in different maize tissues by qPCR. Error bars indicate standard deviations; fold changes are indicated relative to root hairs. *P*-value obtained via Student's t-test, *p*-value *: ≤0.05, n=3. (**c**, **d**) RNA *in situ* hybridization of *rth5* antisense (**c**) and sense (**d**) probes on primary root cross-sections. (**e**-**j**) Immunohistochemistry was performed on cross (**e**, **f**) and longitudinal sections of the differentiation (**g**, **h**) or elongation zone (**i**, **j**). (**e**, **c**, **f**) Sections incubated with anti-RTH5 antibody. (**b**, **d**, **f**) Control sections incubated with buffer. Arrows indicate root hairs. Scale bars in **c**, (**d**) 50 µm, (**e**-**j**) 100 µm. For all experiments in (**c**-**j**) 3-day-old B73 seedling were used.

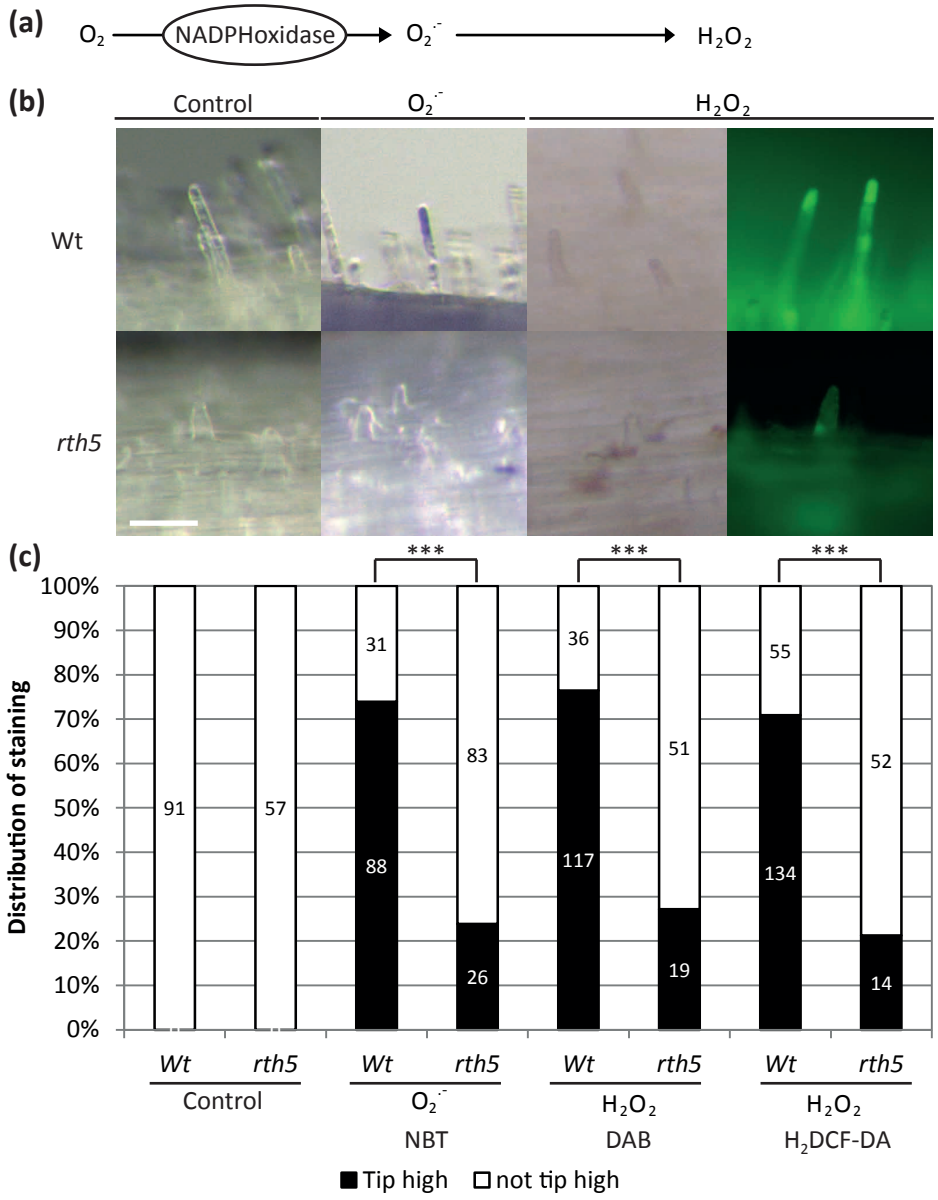

Figure 5. ROS deficiency in *rth5* mutants.
(a) NADPH oxidases superoxide catalyze formation of superoxide which is permutated into hydrogen peroxide. (**b**) ROS staining of wild-type (*Wt*, upper lane) and *rth5* (lower lane) root hairs (from left to right): water control, NBT for superoxide, DAB, and H_2DCF-DA for hydrogen peroxide detection. A GFP filter was used for H_2DCF-DA detection. Scale bar 50 µm. (**c**) Ratio of tip high signals after staining in growing root hairs. Number of analyzed root hairs is indicated in the bars. *P*-values were obtained via Fisher's exact test, *p*-value ***: ≤0.001.

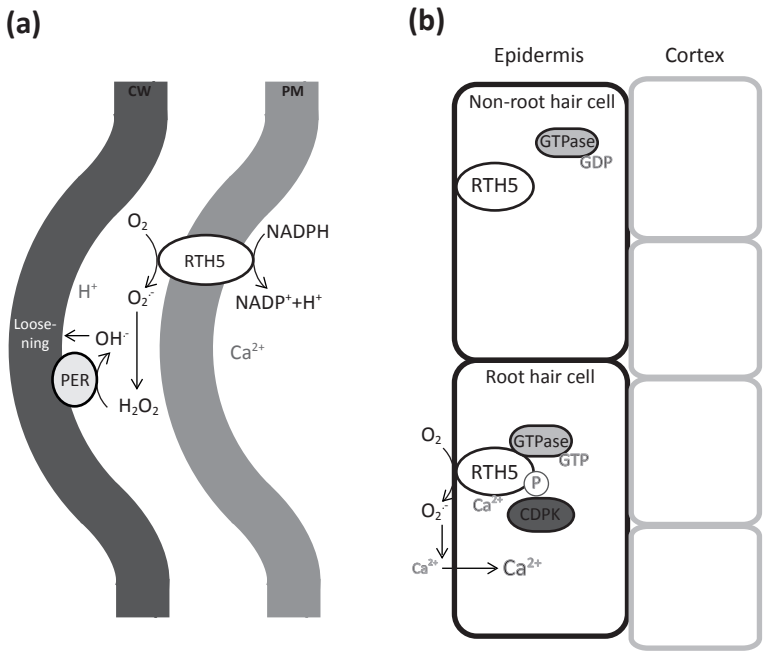

Figure 6. Models for the predicted function of RTH5 in root hair initiation and growth.
(**a**) Illustration of the putative role of RTH5 in tip growth by producing apoplastic superoxide, which is rapidly converted into hydrogen peroxide. Apoplastic peroxidases (PER) generate hydroxyl radicals which are cleaving celluloses and hemicelluloses leading to cell wall loosening. The acidic cell wall (CW) allows oriented growth at the softened site. PM: plasma membrane. (**b**) Suggested function of RTH5 in root hair initiation. A trichoblast-specific signal might activate the RTH5 protein through a small GTPase or calcium-dependent protein kinase (CDPK) to facilitate trichoblast differentiation.

Figure 6